

## Extended Van Hove Singularity in a Noncuprate Layered Superconductor $\text{Sr}_2\text{RuO}_4$

T. Yokoya,<sup>1</sup> A. Chainani,<sup>1</sup> T. Takahashi,<sup>1</sup> H. Katayama-Yoshida,<sup>1</sup> M. Kasai,<sup>2</sup> and Y. Tokura<sup>2,3</sup>

<sup>1</sup>*Department of Physics, Tohoku University, Sendai 980-77, Japan*

<sup>2</sup>*Joint Research Center for Atom Technology (JRCAT), Tsukuba 305, Japan*

<sup>3</sup>*Department of Applied Physics, The University of Tokyo, Tokyo 113, Japan*

(Received 20 June 1995; revised manuscript received 24 October 1995)

Angle-resolved photoemission spectroscopy was performed on a ruthenate superconductor  $\text{Sr}_2\text{RuO}_4$  ( $T_c \sim 1$  K) which has the same crystal structure as  $\text{La}_2\text{CuO}_4$ , but with  $\text{RuO}_2$  layers replacing  $\text{CuO}_2$  layers.  $\text{Sr}_2\text{RuO}_4$  shows an *extended* Van Hove singularity (VHS) at  $20 \pm 2$  meV below  $E_F$  just like the cuprates, regardless of the character of the electronic states at  $E_F$ . This suggests that the *extended* VHS is a general feature of a two-dimensional correlated *d*-electron metal. The observed Fermi surface is in contrast to local-density-approximation calculations.

PACS numbers: 79.60.Bm, 73.20.Dx, 74.72.-h

In understanding the mechanism of superconductivity in high transition temperature (high- $T_c$ ) cuprate superconductors, one of the most important questions today is: Given a pairing force originating in either electron-electron or electron-phonon interactions, or of a more exotic origin, how is the  $T_c$  enhanced to the experimentally observed transition temperatures? Theoretical studies have emphasized the importance of a Van Hove singularity (VHS) arising from a saddle point in the energy-versus-momentum ( $k$ ) relation, which would provide a very high density of states at the Fermi level ( $E_F$ ) as a possible cause for an enhanced  $T_c$  [1]. In a more recent study, the possibility of an electronic pairing mechanism based on the logarithmic VHS has been identified [2]. While there was indirect evidence for the existence of high density of states at  $E_F$  in the cuprates from various experiments [3], only very recent high-resolution angle-resolved photoemission studies have directly observed the VHS near  $E_F$ , possessing a saddle-point topology. Specifically,  $\text{YBa}_2\text{Cu}_4\text{O}_8$  (Y124) exhibits an extended saddle-point singularity derived from energy bands of the  $\text{CuO}_2$  planes positioned at 19 meV below  $E_F$  [4], observed as a sharp peak just below  $E_F$  over a wide range in  $k$  space in angle-resolved photoemission measurements. It was suggested that such an extended singularity could yield a power law divergence in the density of states and could give a  $T_c$  of order 100 K in a weak coupling BCS scheme. Similarly,  $\text{Bi}_2\text{Sr}_2\text{CaCu}_2\text{O}_8$  (Bi2212) and Pr-substituted  $\text{Bi}_2\text{Sr}_2\text{CuO}_6$  (Bi2201) show extended VHS's within 30 meV of  $E_F$  [5,6]. On the other hand,  $\text{Nd}_{2-x}\text{Ce}_x\text{CuO}_4$  (NCCO), the electron doped cuprate, also shows a saddle-point singularity [7], but not of the extended type and positioned far from  $E_F$  ( $\sim 350$  meV). These observations are thought to be consistent with the normal state resistivity which shows a  $T^2$  dependence in NCCO as for a normal Fermi liquid, while the proximity of the VHS to  $E_F$  in the *p*-type high- $T_c$  cuprates has been tied to the linear dependence of the resistivity on temperature. The main purpose of this Letter is to show that (1) the extended VHS is not a preserve

of the cuprates; we observe it in the low- $T_c$  layered superconductor,  $\text{Sr}_2\text{RuO}_4$ ; and (2) while the position of the VHS ( $= 20 \pm 2$  meV, just like the cuprates) and the temperature dependence of crossover from  $T^2$  to  $T$  linear in resistivity seem consistent with the calculations of Newns *et al.* [8], the proximity of a VHS close to  $E_F$  does not guarantee high  $T_c$ . The results suggest that the extended VHS is a general feature of a two-dimensional correlated metal and imply that the high  $T_c$  of the cuprates compared to the ruthenate is derived from an additional mechanism such as a different coupling constant or interlayer coupling between the two systems.

In this study, we present results of high-resolution angle-resolved ultraviolet photoemission spectroscopy (ARUPS) of  $\text{Sr}_2\text{RuO}_4$ . This material has the same crystal structures as  $\text{La}_2\text{CuO}_4$ , but with  $\text{RuO}_2$  planes replacing the  $\text{CuO}_2$  planes. It exhibits superconductivity at 0.93 K [9] and a highly anisotropic resistivity for the in-plane and perpendicular to the plane components, both of which follow a  $T^2$  dependence below 25 K like a typical correlated metal [9,10]. While  $\text{La}_2\text{CuO}_4$  is an antiferromagnetic insulator,  $\text{Sr}_2\text{RuO}_4$  shows enhanced Pauli paramagnetism [11]. A band structure calculation based on the local-density approximation (LDA) to the density functional theory using the linear augmented plane wave method [12] has shown that the  $\text{Ru } 4d\epsilon(xy, yz, zx)\text{-O } 2p\pi$  antibonding bands cross  $E_F$ , while it is well established in the high- $T_c$  cuprates that the  $\text{Cu } 3d_{x^2-y^2}\text{-O } 2p\sigma$  antibonding band crosses the  $E_F$ . Moreover, though the electronic states at  $E_F$  derived from Ru-O antibonding bands have a relatively high density of states giving a specific heat  $\gamma$  value of  $\sim 10$  mJ/K<sup>2</sup> mol, this calculated value is still much less than the observed  $\gamma$  value (39 mJ/K<sup>2</sup> mol) [9]. These observations point to the inadequacy of a simple one-electron picture to account for the properties of  $\text{Sr}_2\text{RuO}_4$ .

Single crystals of  $\text{Sr}_2\text{RuO}_4$  were prepared by the float-zone method. The samples were characterized for structure using x-ray diffraction. Magnetic susceptibility

measurements confirmed the superconductivity at about 0.9 K. ARUPS measurements were performed using a high-resolution angle-resolved photoemission spectrometer constructed at Tohoku University. Samples were cleaved in an ultrahigh vacuum of better than  $4 \times 10^{-11}$  Torr at 20 K. All measurements have also been done at 20 K within 4 h of every cleaving, as the surface degraded beyond 6 h of cleaving as seen by the reduction in intensity of the sharp peak observed near  $E_F$  and a concomitant formation of the well-known contamination or degradation derived feature at about 10 eV binding energy. The contamination-derived feature at 10 eV binding energy is absent only for an atomically clean surface as has been established recently even for Ru oxides [13]. Energy and angular resolutions were 50 meV and less than  $2^\circ$ , respectively. A restricted set of measurements was carried out for the  $\Gamma Z$  direction at higher energy resolution of 30 meV to accurately determine the position of the VHS. The Fermi level was referred to that of a gold film deposited on the sample substrate. The results presented here were acquired from over 15 cleavings and reproducible dispersion was obtained, confirming that the results are intrinsic.

Figure 1 shows the ARUPS spectra of  $\text{Sr}_2\text{RuO}_4$  along the  $\Gamma X$ ,  $\Gamma Z$ , and perpendicular to the  $\Gamma Z$  direction (denoted by  $XX$ ) of the Brillouin zone, measured at 20 K using the He I resonance line ( $h\nu = 21.22$  eV). For the  $\Gamma X$  direction [Fig. 1(a)], we observe two bands located at about 0.1 and 0.4 eV binding energy and  $\theta = 0^\circ$  which is derived from Ru  $4d$  and O  $2p$  antibonding states. These bands approach  $E_F$  for increasing  $\theta$ , before crossing it beyond  $\theta = 16^\circ$  and  $20^\circ$ , respectively. This is understood by the sharp decrease in intensity at  $E_F$  beyond  $\theta = 20^\circ$  and is consistent with crossings expected as in the band

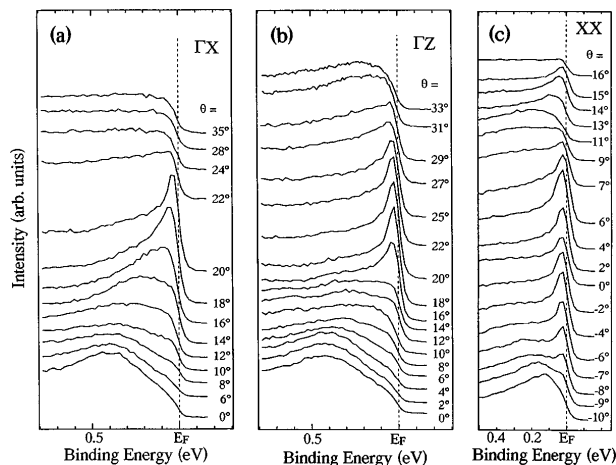


FIG. 1. ARUPS spectra of  $\text{Sr}_2\text{RuO}_4$  in the vicinity of the Fermi level along (a)  $\Gamma X$ , (b)  $\Gamma Z$ , and (c) perpendicular to the  $\Gamma Z$  direction (denoted by  $XX$ ) using He I photons ( $h\nu = 21.22$  eV), measured at 20 K. Also see Fig. 2 for the Brillouin zone and the high-symmetry points of  $\text{Sr}_2\text{RuO}_4$ . The  $\Gamma Z$  direction corresponds to the Ru-O bonding direction.

structure calculation reported by Oguchi [12]. While the crossing at  $16^\circ$  is not clear along the  $\Gamma X$  direction, an independent measurement along the  $c$  direction shows a definite crossing at  $\theta = 16^\circ$  as marked out in Fig. 2 where the  $E_F$  crossings are shown as filled circles. The circles indicate the positions corresponding to the measurement points in the Brillouin zone. For the  $\Gamma Z$  direction, however, the same bands become sharp on approaching  $E_F$  for increasing  $\theta$  and remain as dispersionless sharp peaks at a binding energy of less than 30 meV below  $E_F$  over a wide region of the Brillouin zone [see Fig. 1(b)]. On further increase of  $\theta$ , the feature broadens out and moves again to a higher binding energy, showing that it does not ever cross  $E_F$  along the  $\Gamma Z$  direction. In order to further investigate the nature of the band dispersion near  $E_F$  around the zone boundary, we measured along several lines perpendicular to the  $\Gamma Z$  direction and one special direction parallel to  $\Gamma X$  direction. The corresponding cuts in the Brillouin zone are shown in Fig. 2 as rows of circles labeled  $c, d, e, f,$  and  $g$ . Figure 1(c) shows the result obtained along cut  $e$ . [Note that  $\theta = 0^\circ$  in Fig. 1(c) corresponds to  $\theta = 22^\circ$  in Fig. 1(b).] As can be seen in Fig. 1(c), the narrow peak near  $E_F$  at  $\theta = 0^\circ$  disperses slowly towards  $E_F$  for increasing and decreasing  $\theta$  values and crosses over to unoccupied states at  $\theta = \pm 9^\circ$ , as is evident from the disappearance of the narrow peak at  $E_F$ . Thus, in contrast to a flat maximum observed along the  $\Gamma Z$  direction, the same sharp peak shows a minimum on the  $\Gamma Z$  high symmetry line in a direction perpendicular to it. This behavior is also observed for several cuts perpendicular to the  $\Gamma Z$  direction and the results are summarized in Fig. 3 where we show a surface plot of the dispersion of the singular feature as a function of the in-plane wave vector. As is clearly seen in Fig. 3, the sharp peak near  $E_F$  in  $\text{Sr}_2\text{RuO}_4$

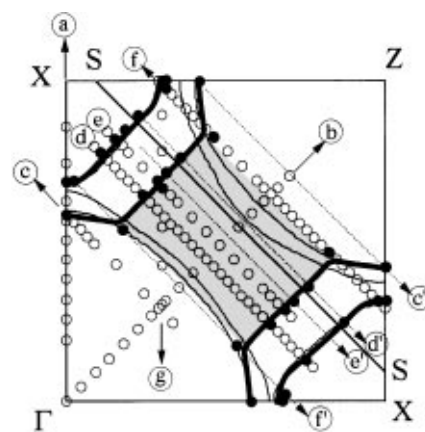


FIG. 2. Section of the calculated [12] (thin line) and observed (thick line) Fermi surface of  $\text{Sr}_2\text{RuO}_4$  together with points in  $k$  space at which ARUPS measurements were performed (circles). Filled circles correspond to  $k$  points at which a band crossing is observed (cuts  $a-g$ ) or expected to be observed (cuts  $c'-f'$ ) from symmetry. Shaded region corresponds to region in which the VHS lies within 30 meV of  $E_F$ .

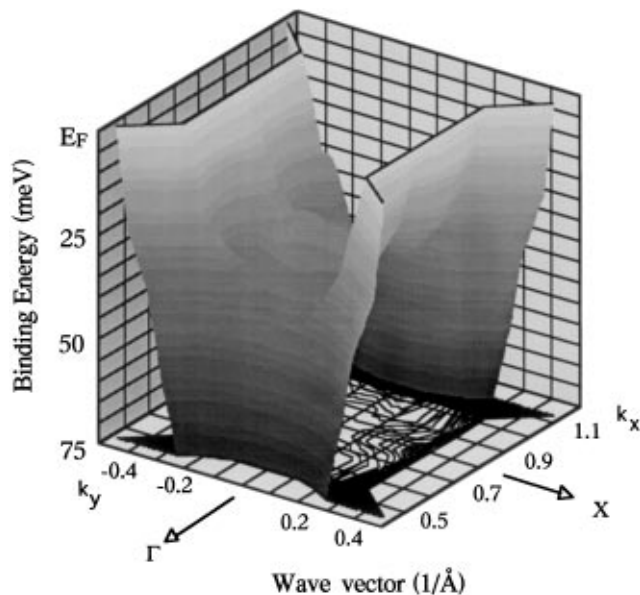


FIG. 3. A surface plot of the dispersion of the singular feature as a function of the in-plane wave vector, showing an extended saddle-point topology. A two-dimensional contour plot is shown in the  $k_x$ - $k_y$  plane.

is a VHS possessing an “extended” saddle-point topology, just as is observed in the high- $T_c$  cuprates [4–6].

In order to check the position of VHS more accurately so as to make comparisons with the VHS observed in the cuprates and to relate with the observed temperature dependence of resistivity, we performed high resolution ARUPS at several points along the  $\Gamma Z$  direction using 30 meV resolution. In Fig. 4, we display these results with the spectra measured at the same  $k$  points with a resolution of 50 meV (Fig. 1). The higher resolution spectra also exhibit the dispersionless sharp peak, i.e., extended VHS, from  $\theta = 16^\circ$  to  $23^\circ$ , in good agreement with the result shown in Fig. 1. But the position of the sharp peak in higher resolution spectra is  $20 \pm 2$  meV in binding energy, closer to  $E_F$  compared to the lower resolution spectra, suggesting the position of VHS is less than or equal to 20 meV. The position of the VHS is thus exactly as is observed in the high- $T_c$  cuprates. The existence of an extended VHS near  $E_F$  in  $\text{Sr}_2\text{RuO}_4$  despite the different character of bands crossing  $E_F$  clarifies the following aspects in relation to the high- $T_c$  cuprates. An extended VHS near  $E_F$  may be a necessary condition for high  $T_c$ , but is surely not a sufficient condition for the same. From a recent angle-resolved photoemission study of a low- $T_c$  ( $\sim 10$  K) cuprate superconductor, King *et al.* [5] conclude that there seems to be no direct relation between a high  $T_c$  and the presence of an extended VHS. As for the present case, the relation between the position of VHS and the temperature dependence of resistivity, Newns *et al.* [8] have shown that the  $T$ -linear resistivity appears only above a temperature of approxi-

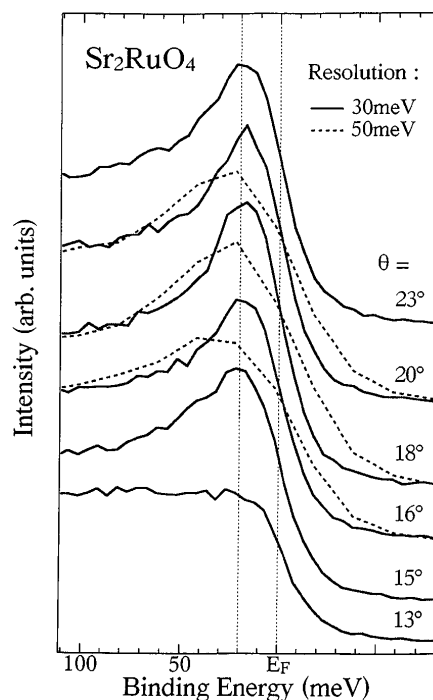


FIG. 4. ARUPS of  $\text{Sr}_2\text{RuO}_4$  using 30 meV energy resolution (solid line) in the vicinity of  $E_F$  obtained at 20 K for several points along the  $\Gamma Z$  line. Broken lines are ARUPS using 50 meV resolution measured at the same  $k$  points. Note that positions of the sharp peaks of high-resolution spectra are about  $20 \pm 2$  meV, which is closer to  $E_F$  than those of low-resolution spectra, indicating that the VHS lies at or less than 20 meV from  $E_F$ .

mately  $\frac{1}{4}$  of the energy position of VHS. The position of VHS (20 meV–230 K) then suggests that the resistivity should exhibit  $T^2$  behavior below about 60 K and is in fair agreement with experiments which show  $T^2$  dependence below 25 K and a crossover to  $T$ -linear resistivity by about 100 K.

Finally, we discuss the Fermi surface topology of  $\text{Sr}_2\text{RuO}_4$ . Figure 2 shows the experimentally obtained Fermi surface (thick line) compared with that obtained from LDA calculations (thin line). Filled circles along the cuts  $a$ ,  $c$ ,  $d$ ,  $e$ ,  $f$ , and  $g$  are observed Fermi surface crossings and those along  $c'$ ,  $d'$ ,  $e'$ , and  $f'$  are expected crossings from symmetry. The calculated surface shows two electron pockets centered at the  $\Gamma$  point and a hole pocket around the  $X$  point. While the hole pocket expected around the  $X$  point is observed experimentally, the two electron pockets are not observed. Instead, we observe an additional hole pocket around the  $X$  point. Though the possibility of an electron pocket around the  $\Gamma$  point cannot be ruled out with the present resolution, the observed Fermi surfaces with two hole pockets are in strong contrast to the LDA calculations. Our results seem consistent with the observation that the Hall coefficient is positive from room temperature up to about 10 K

though it changes sign below 10 K [14]. However, a recent de Haas-van Alphen (dHvA) effect measurement [15] has observed three Fermi surfaces as in the LDA calculations, though the nature of the Fermi surfaces being electron or hole type cannot be addressed by dHvA measurements. A possible explanation for the different Fermi surface observed in this study is that the surface potential could change the electron count at the surface and would make the Fermi surface topology different from that in the bulk. The possibility of a change of Fermi surface topology and a VHS along the  $\Gamma Z$  direction, but with a rigid band shift of approximately 0.2 electron, has been suggested by Singh [16]. But even in that case, the VHS is not of the extended type. Another explanation is that strong correlations change the band structure substantially, as is also supported from transport and magnetic measurements as well as a recent valence band resonant photoemission study [17] across the  $4p-4d$  threshold which has identified the presence of a correlation induced satellite of the  $d$  band.

In conclusion, the similar nature of the extended VHS in  $\text{Sr}_2\text{RuO}_4$  and the high- $T_c$  cuprates regardless of the origin of the electronic states at  $E_F$  imply that the extended VHS is a general and characteristic feature of the electronic structure of two-dimensional correlated  $d$ -electron systems. On the other hand, the large difference of the superconducting transition temperature between  $\text{Sr}_2\text{RuO}_4$  and the cuprates requests a reexamination of the VHS scenario and its relation to superconducting properties. The observed Fermi surface is in contrast to the LDA calculations. Further work on  $\text{Sr}_2\text{RuO}_4$ , in particular, neutron-scattering and/or nuclear-magnetic resonance studies to check for short-range antiferromagnetic correlations as the possible origin for the VHS [18], would be well worthwhile in understanding the phenomena of high- $T_c$  superconductivity.

We thank Y. Maeno for useful discussions and performing the ac susceptibility measurements. We also thank Professor Tachiki for valuable discussions. T. Y. and A. C. thank the Japan Society for the Promotion of Science for financial support. This work was supported by grants from the Ministry of Education, Culture and

Science and the New Energy and Industrial Technology Development Organization (NEDO) of Japan.

- 
- [1] P. Horsch and H. Rietschel, *Z. Phys. B* **27**, 153 (1977); J.E. Hirsch and D.J. Scalapino, *Phys. Rev. Lett.* **56**, 2732 (1986); J. Labbe and J. Bok, *Europhys. Lett.* **3**, 1225 (1987); P.A. Lee and N. Read, *Phys. Rev. Lett.* **58**, 2691 (1987); J. Friedel, *J. Phys. Condens. Matter* **1**, 7757 (1989); R.S. Markiewicz, *Int. J. Mod. Phys. B* **5**, 2037 (1991).
  - [2] D.M. Newns, H.R. Krishnamurthy, P.C. Pattnaik, C.C. Tsuei, and C.L. Kane, *Phys. Rev. Lett.* **69**, 1264 (1992).
  - [3] C.C. Tsuei, D.M. Newns, C.C. Chi, and P.C. Pattnaik, *Phys. Rev. Lett.* **65**, 2724 (1990), and references therein.
  - [4] K. Gofron *et al.*, *J. Phys. Chem. Solids* **54**, 1193 (1993); A.A. Abrikosov, J.C. Campuzano, and K. Gofron, *Physica (Amsterdam)* **214C**, 73 (1993); K. Gofron *et al.*, *Phys. Rev. Lett.* **73**, 3302 (1994).
  - [5] D.S. Dessau *et al.*, *Phys. Rev. Lett.* **71**, 2781 (1993); D.M. King *et al.*, *Phys. Rev. Lett.* **73**, 3298 (1994).
  - [6] Jian Ma *et al.*, *Phys. Rev. B* **51**, 3832 (1995).
  - [7] D.M. King *et al.*, *Phys. Rev. Lett.* **70**, 3159 (1993).
  - [8] D.M. Newns, H.R. Krishnamurthy, P.C. Pattnaik, C.C. Tsuei, C.C. Chi, and C.L. Kane, *Physica (Amsterdam)* **186B**, 801 (1993).
  - [9] Y. Maeno, H. Hashimoto, K. Yoshida, S. Nishizaki, T. Fujita, J.G. Bednorz, and F. Lichtenberg, *Nature (London)* **372**, 532 (1995).
  - [10] F. Lichtenberg, A. Catana, J. Mannhart, and D.G. Schlom, *Appl. Phys. Lett.* **60**, 1138 (1992).
  - [11] J.J. Neumeier *et al.*, *Phys. Rev. B* **50**, 17910 (1994); R.J. Cava *et al.*, *Phys. Rev. B* **49**, 11890 (1994).
  - [12] T. Oguchi, *Phys. Rev. B* **51**, 1385 (1995).
  - [13] A. Gulino, R.G. Egdell, P.D. Battle, and S.H. Kim, *Phys. Rev. B* **51**, 6827 (1995); P.A. Cox, R.G. Egdell, J.B. Goodenough, A. Hamnett, and C.C. Naish, *J. Phys. C* **16**, 6221 (1983).
  - [14] N. Shirakawa *et al.*, *J. Phys. Soc. Jpn.* **64**, 1072 (1995).
  - [15] A.P. Mackenzie *et al.* (private communication).
  - [16] David J. Singh, *Phys. Rev. B* **52**, 1358 (1995).
  - [17] T. Yokoya *et al.*, *Phys. Rev. B* (to be published).
  - [18] E. Dagotto, A. Nazarenko, and A. Moreo, *Phys. Rev. Lett.* **74**, 310 (1995).